Performance of light-frame shear wall framed with Japanese lumber

Anthony Newton
Graduate Research Assistant
Department of Wood Science & Engineering
Oregon State University, Corvallis, OR 97331
Email: anthony.newton@oregonstate.edu

Tyler Deboodt
Senior Faculty Research Assistant
Department of Wood Science & Engineering
Oregon State University, Corvallis, OR 97331
Email: tyler.deboodt@oregonstate.edu

Yuichi Sato
Managing Director
Japan Lumber Inspection and Research Association, JLIRA
2-3-13 Kanda Ogawamachi,
Chiyoda-ku, Tokyo, 101-0052 JAPAN
sato@jlira.jp

Arijit Sinha *†
Professor & JELD-WEN Chair
Department of Wood Science & Engineering
Oregon State University, Corvallis, OR 97331
Email: Arijit.sinha@oregonstate.edu

(Received 26 January 2026)

Abstract: Recently, Hinoki and Sugi, two predominant wood species in Japan, had approval for their design values to be listed in the National Design Specification for wood-frame construction in the United States. However, their ability to meet the demands of a light-framed shear wall has not been studied. The objective of this study was to characterize the behavior of Hinoki and Sugi framed shear walls with conventional sheathing material, and compare the performance to Douglas-fir framed shear walls. Twelve light-frame shear walls were constructed, and one monotonic and three cyclic tests were performed per wall type consisting of Douglas-fir, Hinoki, and Sugi. Hinoki showed similar properties to that of Douglas-fir, while Sugi observed a lower lateral resistance and stiffness compared to the Douglas-fir. All walls in this study met seismic equivalent parameters, which allow the wall configurations used in this study to be compared to other wood-frame sheathed wall types.

Keywords: Shear wall; Light-frame; Seismic performance; Hysteresis; EEEP.

Introduction

Wood light-frame construction, referred to as wood-framed construction from here on, represents approximately 94% of residential houses constructed in the United States in 2021 (Fu 2025). An important aspect of wood-frame construction is the design and performance of a shear wall, which is an integral component of the lateral force resisting system (LFRS). Shear walls are typically framed with dimension lumber with structural sheathing (such as oriented strand board and plywood) fastened to the frame using nails and other mechanical fasteners. To regulate the performance of these buildings, the International Residential Code (IRC) (International Code Council 2020) provides prescriptive building designs to ensure that minimum performance standards are met. However, to obtain unit shear capacities and design values of these shear walls, the "Special Design Provisions for Wind and Seismic" (SDPWS) standard, published by American Wood Council, is used. Because Sugi (*Cryptomeria japonica*) and Hinoki (*Chamaecyparis obtusa*) are widely used in Japanese construction and originate from a region with seismic demands comparable to those in the US, evaluating their performance within US light-frame design standards provides important context for their potential use in domestic construction.

Planted forests account for approximately 40% of Japan's total forest area (Ministry of Agriculture, Forestry and Fisheries 2023). Among these, Sugi is the most extensively planted

* Corresponding author
† Society of Wood Science & Technology member

https://doi.org/10.22382/wfs-2026-15

species, followed by Hinoki, reflecting their long-standing importance in Japan's timber supply. Following World War II, Japan faced a critical need for construction materials, which led to large-scale harvesting, the rapid establishment of reforestation programs, and widespread planting of Sugi and Hinoki to support the nation's rebuilding efforts. Today, forestry remains a significant industry, with a total output of 580.7 billion yen in 2022 (approximately 3.464 billion USD). About 80% of low-rise residential buildings in Japan are constructed from wood, underscoring the continued dominant use of these species in the built environment. Japan, like the Pacific Coast of the United States, is located in a high seismic risk zone, further emphasizing the relevance of understanding the structural performance of Sugi and Hinoki for modern construction practices.

Given the extensive use of Sugi and Hinoki in Japan's planted forests and their prominence in Japanese residential construction, it is important to understand how these species perform when used in structural systems common in the United States. In typical shear wall framing, any species listed in the American Wood Council (AWC) National Design Specification (NDS) Supplement (AWC 2024) can be used. With the recent introduction of Sugi and Hinoki into the US construction market through their acceptance into the NDS (American Wood Council 2024), there is a need to characterize their performance as framing materials in shear wall applications. Furthermore, comparing their behavior with that of Douglas-fir (*Pseudotsuga menziesii*), a commonly used US framing species, can provide essential information that may support broader adoption of Sugi (*Cryptomeria japonica*) and Hinoki (*Chamaecyparis obtusa*) within the US construction sector.

During an earthquake, ground shaking and ground failure are the primary contributors to loss of life and property. This was evident during the Northridge earthquake on January 17, 1994. The Los Angeles metropolitan area experienced significant damage to wood-frame construction, which was categorized into three main areas: casualties, property loss, and loss of functionality (Krawinkler et al. 2001). In response, the CUREE-Caltech Woodframe Project was launched to combine research and practical implementation to enhance the seismic resistance of wood-frame buildings. Through the Consortium of Universities for Research in Earthquake Engineering (CUREE), a standard testing protocol was created for component tests. Representative loading histories were developed based on the seismic demands placed on wood buildings during California earthquakes. This included the development of a protocol for displacement-controlled quasi-static reverse cyclic testing.

In low-rise wood structures, shear walls act as the primary LFRS. These consist of dimensional lumber framing combined with plywood, oriented strand board (OSB), or other sheathing materials capable of resisting shear forces acting on the assembly. Shear walls are primarily connected using nails; the sheathing resists lateral forces, while the framing supports vertical gravity loads. This combination contributes to overall rigidity and limits deflection. Van de Lindt (2004) highlights two characteristics that enable light-frame wood structures to perform well during moderate and severe ground shaking: their high strength-to-weight ratio and their ability to dissipate energy through the accumulation of individual fastener deformations.

Standard racking tests have been used since the 1940s to determine the shear strength of wood shear walls. These tests have undergone considerable evolution, including protocols developed under the CUREE project. Research has revealed key insights, for example, the critical influence of shear wall-to-framing connections on structural behavior (Cheung et al. 1988), and the comparable shear capacities of plywood and OSB as sheathing materials (Serrette et al. 1997). Van de Lindt (2004) provides a comprehensive review of shear wall testing and its evolution over time. Since 2004, several other studies have characterized shear wall systems. Sinha and Gupta (2009) investigated the contribution of gypsum wallboard to the overall performance of shear walls. Seaders et al. (2009) examined the performance of wood-frame shear walls under monotonic and cyclic loading, including comparisons of partially and fully anchored configurations. Way et al. (2019) investigated the performance of light-frame shear walls with weathered sheathing. Bagheri and Doudak (2020) evaluated the characteristics of shear walls with various construction details, identifying the effects of different wall types on structural performance. Key research advances on characterizing the performance of shear walls constructed with Sugi has been reported in Japan. Shear wall systems constructed with Sugi have demonstrated favorable lateral performance, including adequate strength, deformability, and energy dissipation capacity, in both traditional and contemporary timber construction in Japan (Okazaki and Watanabe 2005). However, much of the foundational experimental and analytical work on Sugi-based shear walls remains published in Japanese-language journals, technical reports, and conference proceedings (Mori et al. 2005; Inayama 2003) limiting accessibility and broader dissemination within the international research community. As a result, despite a body of knowledge on wall system performance, these findings are often underrepresented in global design frameworks and comparative studies. Greater synthesis and translation of this literature are needed to enable more rigorous benchmarking and to facilitate the integration of Sugi-based systems into international timber engineering practice. ASTM E564, Standard Practice for Static Load Test for Shear Resistance of Framed Walls for Buildings (ASTM International 2018), evaluates the capacity of a typical framed wall section, using a rigid foundation and applying a static load parallel to the base at the opposite edge. Later, ASTM developed method E2126, Test Methods for Cyclic (Reversed) Load Test for Shear Resistance of Vertical Elements of the Lateral Force Resisting Systems for Buildings (2019), which provides a standardized cyclic loading test to assess the shear resistance of vertical components in LFRS assemblies. To demonstrate equivalency between various wood-frame shear walls, ASTM introduced D7989, Standard Practice for Demonstrating Equivalent In-Plane Lateral Seismic Performance to Wood-Frame Shear Walls Sheathed with Wood Structural Panels (2021), which includes seismic equivalency parameters (SEPs). The SEPs were developed by an International Code Council (ICC) Evaluation Service task group and are used to demonstrate seismic equivalency for new structural systems. These are calculated using allowable stress design (ASD) values derived from SDPWS.

The objectives of this study are to

1. Characterize the performance of shear walls built with Hinoki and Sugi framing.
2. Investigate the difference in behavior between Hinoki, Sugi, and Douglas-fir framing with full-scale monotonic and cyclic lateral testing.
3. Compare the performance of each shear wall type to other wood-frame sheathed wall types.

Materials and methods

Wall specimen

Wall specimens were designed based on the 2021 International Residential Code (IRC) prescribed brace panel construction. Walls were designed at 2440 × 2440 mm (8 ft × 8 ft) sections, as shown in Figure 1. Fastener details for all three wall types are provided in Table 1.

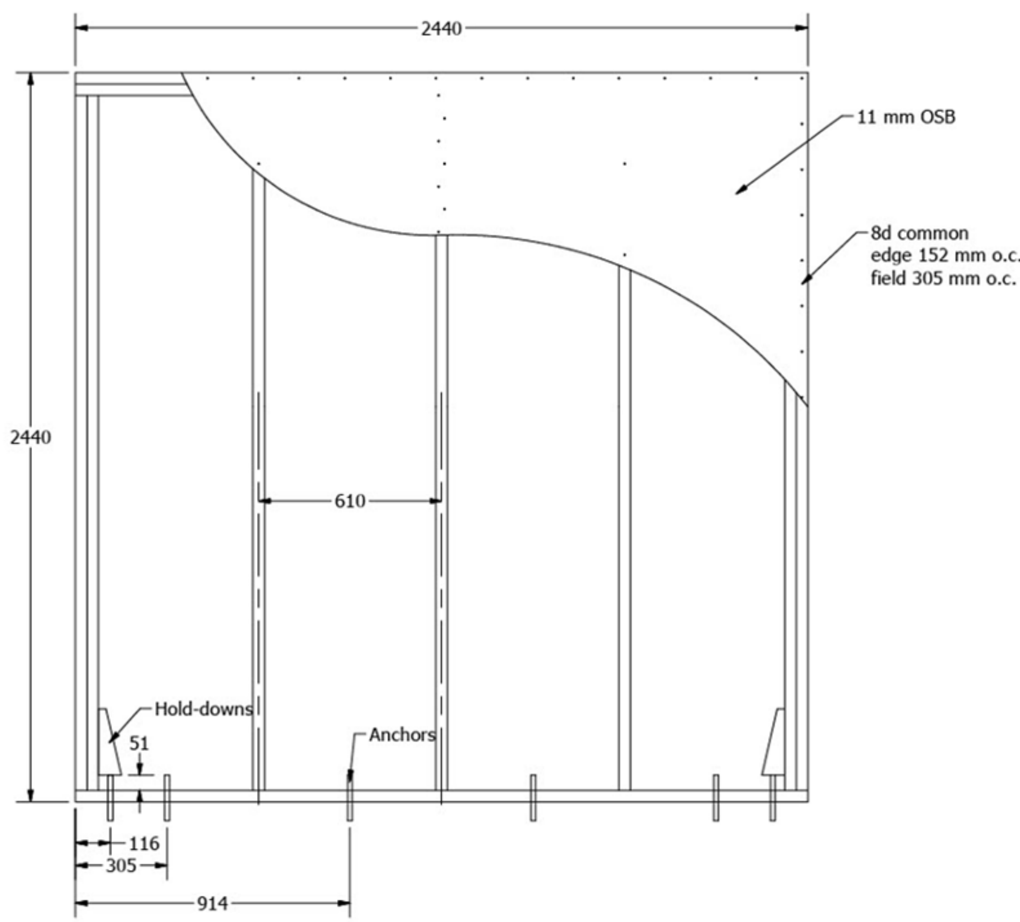

Figure 1. Schematic of wood-frame shear wall.

Table 1. Fastener details and schedule for walls tested.

Details	Type	Description
Framing material	No. 2 graded, 38 × 140 mm	Douglas-fir, Sugi, Hinoki
Sheathing material	OSB	11.1 mm thickness, 24/16 rated
Fasteners	8d common – 3.32 mm dia; 63.5 mm length	Sheathing
	10d box – 3.32 mm dia; 76 mm length	Stud to Stud
	16d common – 3.33 mm dia; 82.5 mm length	Framing
Fastener spacing	152 mm	Edges
	304 mm	Field

For each species used, the board size and grade was 38 × 140mm (2×6) graded No. 2 boards. Studs were spaced at 610 mm (24 in.) on center; these were fastened to the top and bottom plates with 2-16d common end nails (3.33 mm dia × 82.55 mm length; 0.131 in dia × 3.25 in length). Double studs and double plates were fastened together using 2-10d box nails (3.32 mm dia × 76 mm length; 0.131 in dia × 3 in length) every 406 mm (16 in.). Two structural OSB boards (1220 mm width × 2440 mm length × 11.1 mm thickness; and 48 in width × 96 in length ×7/16 in thick) were used with a span rating of 24/16. Sheathing was fastened using 8d common nails at 152 mm (6 in.) on center around the edges of the panel and at 305 mm (12 in.) in the panel field. All nails were smooth shank and were fastened using a Bostitch pneumatic nail gun. Four 19 mm (0.75 in.) anchor bolts (grade 5) were placed along the sill plate with Simpson bearing plates BP 5/8-2 (51 mm width × 51 mm length x 4.76 mm thick; 2 in width × 2 in width × 0.1875 in thick). Two Simpson HDU hold-downs (221 mm; 8.6875 in.) were attached 2 inches above the sill plate on the inside face of the end studs and fastened using Strong-Drive SDS Heavy Duty Connector screws (6.35 mm dia × 63.5 mm length; 0.25 in dia × 2.5 in length) with the use of a Hilti impact driver.

Load frame and test equipment

All tests were conducted at the Gene D. Knudson Wood Engineering Laboratory at Oregon State University. The loading frame used for monotonic and cyclic testing is shown in Figure 2.

The bases of the walls were bolted to a steel beam that was attached to a strong floor to simulate a fixed foundation. Attached to the strong wall was a 490 kN (110 kip) servo controlled hydraulic actuator with 254 mm (10 in.) total of stroke used to apply force to the top of the wall. To allow vertical movement of the actuator while relieving its gravity load on the wall, it was supported by a vertical 102 mm (4 in.) hydraulic cylinder.

Figure 2. Test set up.

The supporting piston utilizes a 111.2 kN (25 kip) load cell for force measurements. The steel C-channel was attached to the top of the wall with four 22 mm (0.87 in.) short-threaded rods (ASTM F1554 grade 36) across the top of the wall. To prevent out-of-plane movement, two steel poles were laterally braced from the strong wall to the C-channel.

Testing protocol

Monotonic tests

Monotonic tests were based on the ASTM E564-06 (ASTM International 2018) test protocol, which was used to determine static load capacity and deflection of framed wall sections. This protocol required the ultimate load to be reached in no less than 5 minutes. Loading rate of monotonic test was 0.21 mm/sec (0.008 in./sec). Using this testing method, a monotonic deformation capacity (Δ_m) was derived; this deformation capacity was equal to the distance that a wall deflects for the first time below 80% maximum load.

Cyclic tests

Cyclic tests followed ASTM E2126-19 (ASTM International 2019) Test Method C, also known as the CUREE Basic Loading Protocol as shown in Figure 3. This protocol is designed to simulate the deformation demands that vertical elements of a lateral force resisting system (LFRS) may experience under lateral loads (such as wind or seismic forces). The CUREE protocol required a reference displacement (Δ_{ref}), which is 60% of monotonic deformation capacity ($\Delta_{ref} = 0.6*\Delta_m$) to build a series of increasing deformation cycles. This loading protocol consisted of three types of cycles: initial cycles, primary cycles, and trailing cycles. Loading began with six initial cycles at small amplitudes equal to 5% of the reference displacement. These were followed by the primary cycles, with the first primary cycle applied at 7.5% of the reference displacement. Subsequent primary cycles increased in amplitude, progressing up to 2 times the reference displacement. After each primary cycle, a trailing cycle was applied at an amplitude equal to 75% of the displacement of the preceding primary cycle. In the full protocol, primary cycles continued to increase in increments of 0.5 times the reference displacement, beyond 2 times the reference displacement; however, in this study, loading was only required up to 2 times the reference displacement.

Test matrix

Testing consisted of three different species (Douglas-fir, Hinoki, and Sugi) under two different loading conditions (monotonic and cyclic). Three walls were tested in monotonic, and nine walls were tested in cyclic loading. One monotonic test was required to gain the reference displacement for each wall type, while the number of tests for cyclic was in accordance with ASTM E2126 (ASTM International 2019). In accordance with the standard, only two cyclic tests are required for a given wall configuration; however, the standard also specifies that a third test must be conducted when the difference in peak load between the first two tests exceeds 10%. For this reason, a third wall was tested in this study. Table 2 shows the complete listing of the testing and the labeling used for each wall type.

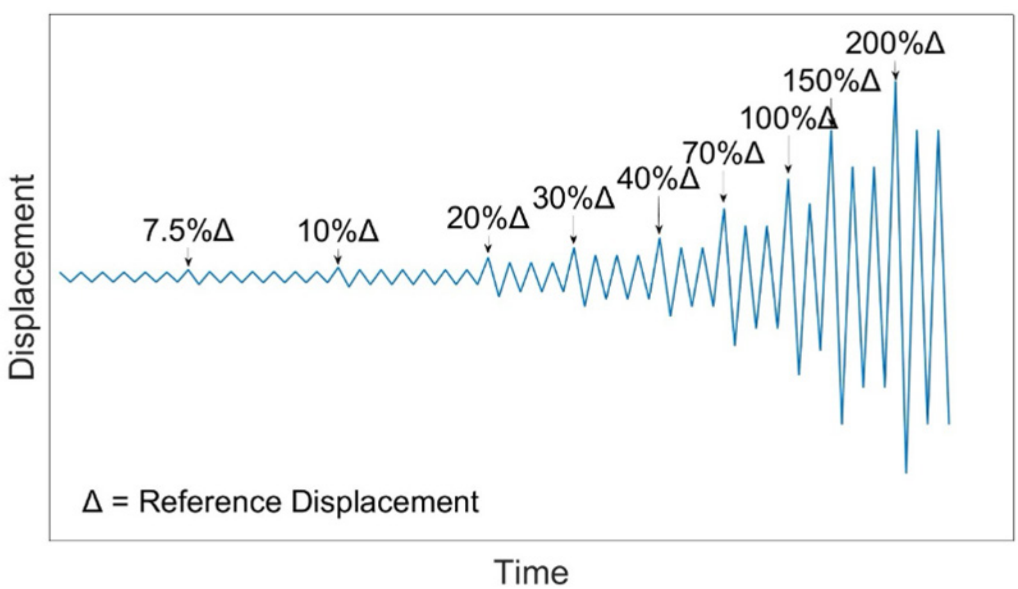

Figure 3. Cyclic loading protocol.

Table 2. Test matrix.

Wall type	Monotonic	Cyclic
Douglas-fir	1	3
Hinoki	1	3
Sugi	1	3

Data Acquisition

Multiple measurements were made during testing to help characterize the performance of the walls. These measurements included force applied along the top-plate, displacement of the top-plate, uplift that occurred at each end stud, and slip that occurred at the sill plate. Force applied was measured using an Interface High-Capacity Fatigue-Rated Universal Low-profile load cell. The load cell's capacity is 450 kN (100 Kip); in use of hysteresis, its accuracy was ±0.06% full scale. Displacement of the top of the wall was measured by an internal displacement sensor in the actuator, as well as a string potentiometer attached to the top plate and the opposite end of the wall. For calculations, the string potentiometer displacement was used to reduce error in displacement that could have been caused by slipping between the top-plate and the attached steel beam. The string potentiometer was a Micro-epsilon wire sensor, WDS-P60, with a measuring range of 300 mm (11.8 in.), with a linear accuracy of ±0.1% full scale output. To measure the uplift of the wall, one linear variable differential transformer (LVDT) was placed at each end of the wall approximately 127 mm (5 in.) from the ground. The LVDT had a range of ±12.7 mm (0.5 in.) with an accuracy of 0.25% of its full stroke. To measure the slip of the sill plate, a LVDT was used with a range of ±7.62 mm (0.3 in.), with an accuracy of 0.25% of its full stroke.

Load-displacement curves

To present the structural behavior of the shear walls, a load displacement curve or load envelope is commonly employed. For monotonic tests, the acquired load was directly plotted from the observed load-displacement data. From the cyclic tests, hysteresis was acquired. To gain a more representative figure and one that could be compared to that of monotonic testing, an envelope curve was derived. The envelope curve was made up of maximum forces reached at every primary cycle in both directions. From these, we gained a positive and negative envelope curve that could be averaged to show a representative load-displacement curve that can be compared with monotonic test. From the average envelope, an equivalent energy-plastic (EEEP) curve can be calculated.

Table 3. EEEP parameters.

Parameters	Units	Description
P_{yield}	kN	Yield load
E	kN•mm	Energy under back bone curve up to failure
P_{peak}	kN	Maximum load in a given envelope
Δ_e	mm	Displacement of specimen at $0.4{*}P_{peak}$
K_e	kN/mm	$0.4{*}P_{peak}/\Delta_{e;}$ Initial stiffness

EEEP curve

All parameters of the EEEP curve were derived from the envelope curve and are listed in Table 3, and were calculated as per ASTM D2126 (2019)

The initial portion of the EEEP curve is the initial stiffness of the wall. This initial stiffness (K_0) is equal to 40% of the maximum load over the displacement that it took to reach said load. Due to the non-linear behavior of lateral loading in wood shear walls, an alternative to traditional ductility was determined. The alternative was the absorbed energy (E), calculated as the area enclosed under the monotonic and envelope curves, up to the deformation capacity.

Yield load is calculated as per Eq. 1,

$$P_{yield} = \left(\Delta_u^2 - \sqrt{\Delta_u^2 - \frac{2E}{K_e}}\right)K_e \qquad [1]$$

Where, Δ_u is the ultimate displacement, E is the energy under the curve up to failure; K_e is the initial stiffness.

Post-testing

After testing, moisture content for each wall was measured using two different methods, selected based on the species of wood. For the Douglas-fir walls, a pin-type moisture meter was used, with four readings taken at different locations on each wall and then averaged. For the Hinoki and Sugi walls, moisture content was determined using the oven-dry method Small sections of framing were removed from each wall and placed in a dry oven set to 103°C ± 2°C for 24 hours and weighed before and after drying.

Results and Discussion

Monotonic testing

Load-displacement curves from monotonic testing for the three wall types are shown in Figure 4. Peak load of the three wall

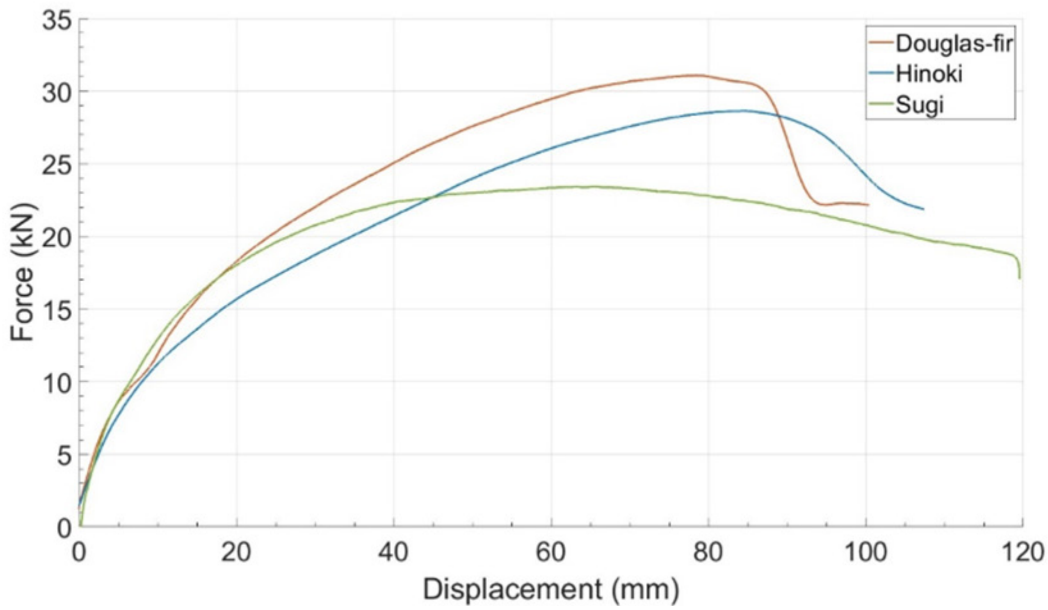

Figure 4. Load -displacement response from monotonic tests.

types were as follows: 31.85 kN (7160 lbf) for the Douglas-fir wall; 29.51kN (6634 lbf) for the Hinoki wall; and 23.00 kN (5170 lbf) for the Sugi wall. The main contributor to peak force is the sheathing type and amount of panel to stud nails. However, a 28% decrease in strength in comparison with the Sugi to Douglas-fir [Specific Gravity (SG) = 0.50] was observed and can be attributed to the lower density of Sugi (SG = 0.36). The SG of Sugi is 28% lower than that of Douglas-fir. This also can account for its lower stiffness in comparison to both Douglas-fir and Hinoki (SG = 0.45).

The ultimate displacement is the point of the linear curve where the force reaches 80% of the peak force for the first time after peak load had been reached. Douglas-fir reached its ultimate displacement at 82.7 mm (3.25 in.), while Hinoki reached it at 101 mm (3.98 in.), and Sugi at 110 mm (4.33 in.). These values were used to calculate the Δ_{ref}. Results from the Douglas-fir and Hinoki monotonic test were averaged to determine Δ_{ref}. The reference displacement values from each test were 49.5 mm (1.95 in.) for Douglas-fir and 60.5 mm (2.38 in.) for Hinoki. For cyclic testing, the two were averaged and rounded to 56 mm (2.2 in.). During the monotonic test for Sugi, the measured Δ_{ref} was 66.14 mm (2.60 in.). However, to account for the larger ultimate displacement exhibited by Sugi and to remain within the actuator's stroke limit of ±5 in, a reference displacement of 61 mm (2.4 in.) was selected. The purpose of this change was to allow the Sugi specimens to have a greater displacement at the final cycles of the test and reach a failure point.

Cyclic testing

Cyclic tests were done in accordance with ASTM E2126-19 (ASTM International 2019). The hysteresis loops for all tests are shown in Figure 5. It is noted that the positive direction showed higher strength and stiffness than the negative cycle. The higher resistance observed under positive loading compared with negative loading is likely associated with the cumulative effects of reversed cyclic loading. Under repeated load reversals, localized damage mechanisms such as embedment, slip, gap evolution, and progressive inelastic deformation can accumulate, resulting in degradation of both stiffness and peak resistance. Because the response in one loading direction is influenced by damage sustained during prior excursions in the opposite direction, the lower negative-direction resistance likely reflects a more degraded structural state of the specimen rather than an intrinsic directional strength difference alone. Thus, the asymmetry in resistance is better interpreted because of cyclic damage accumulation and load-history-dependent degradation of the force-transfer mechanism.

Douglas-fir (Figure 5a) and Hinoki (Figure 5b) had similar behavior, while Sugi (Figure 5c) had a lower stiffness. The differences in stiffness between the Sugi and the other two

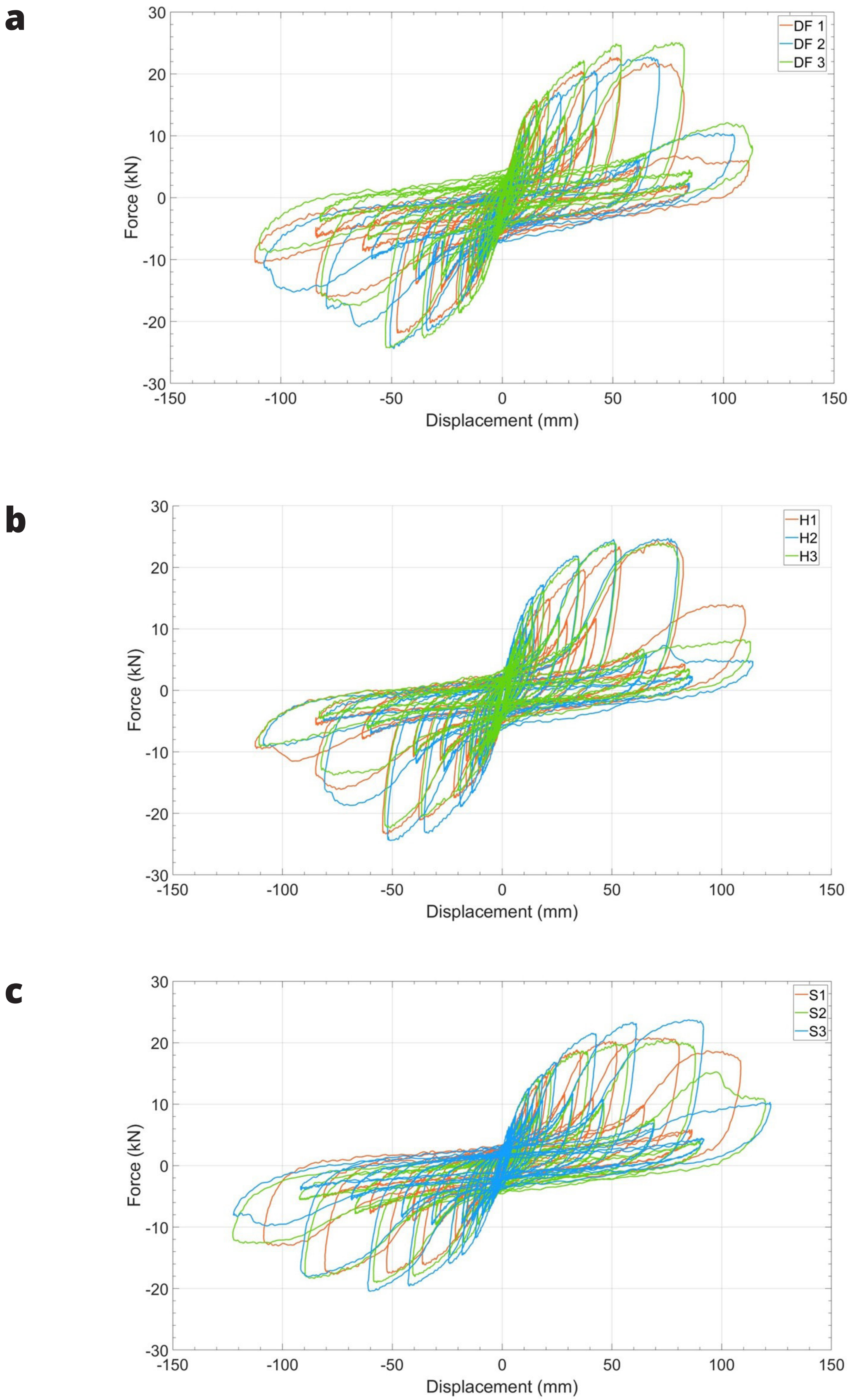

Figure 5. Typical hysteresis of wall tested (a) Douglas-fir; (b) Hinoki; and (c) Sugi.

species can be attributed to the differences in specific gravity of the framing material.

While Sugi demonstrated a larger displacement capacity in monotonic testing, an initial attempt was made to use the same reference displacement as Douglas-fir and Hinoki for the first Sugi cyclic test. However, failure, defined in ASTM E2126 (ASTM International 2019) as the point where the lateral resistance drops to 80% of the peak load, was not reached in this test. As a result, a larger reference displacement was adopted for the subsequent two cyclic tests to ensure that failure was achieved. The initial Sugi cyclic test was still included in the species comparison, and for this specimen the ultimate displacement was taken as the last point on the envelope curve rather than an interpolated point corresponding to 80% of peak load, as permitted by ASTM E2126. The average envelope curve, shown in Figure 6, represents the mean backbone response derived from both the positive and negative loading segments of the hysteresis loops for each species. Further presented in Figure 6 are the monotonic curves for direct comparison of each wall species.

Based on average envelopes from across tested species, the shear capacity of the Douglas-fir wall type was 9.56 kN/m (655 lb/ft), while the Hinoki wall type was 9.76 kN/m (669 lb/ft), and the Sugi wall type was 8.69 kN/mm (595 lb/ft). Douglas-fir and Hinoki walls reached their maximum resistance at lower drift levels, while the Sugi wall exhibited its peak force at a noticeably larger drift. This behavior is reflected in the envelope curves shown in Figure 6. In general, direct comparison between monotonic and cyclic envelope responses reveals that the monotonic tests exhibited higher peak resistance and greater initial stiffness. This difference arises from the absence of load reversals in monotonic loading, which limits the accumulation of inelastic damage. Under cyclic loading, repeated reversals induced progressive degradation mechanisms, including localized crushing, interfacial slip, and gap evolution, leading to stiffness reduction, pinching behavior, and diminished peak resistance. As a result, the cyclic envelope curve reflects a degraded response that incorporates cumulative damage effects, whereas the monotonic response represents an upper-bound capacity under a single loading path.

Results from monotonic tests can be compared to the Seaders et al. (2009) fully anchored monotonic and cyclic results, since they used a construction geometry exactly similar to this study, with the only difference being Douglas-fir framing and 11-mm thick OSB as sheathing. The average peak force of the monotonic walls for this study was 15% greater than that of Seaders et al. (2009), while the cyclic average response was 2.5% greater. The EEEP presented in Figure 7 were derived

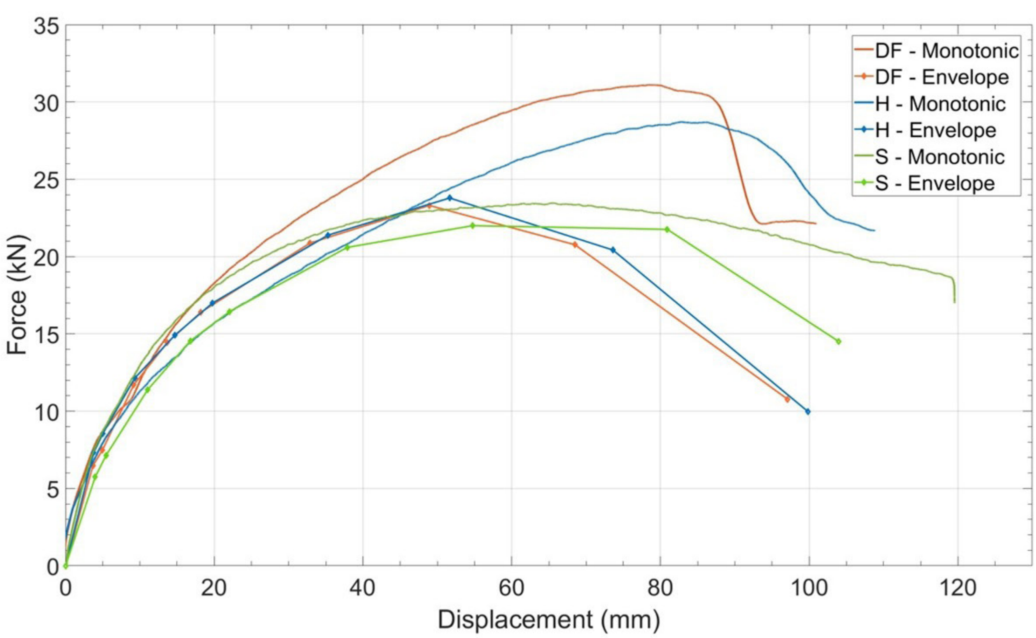

Figure 6. Average envelope curves for the tested wall types.

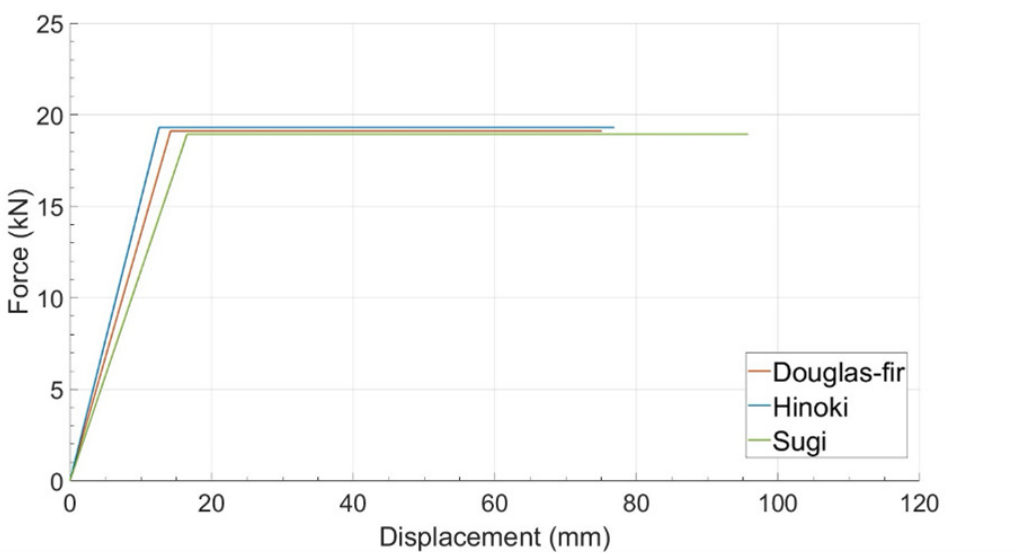

Figure 7. Average equivalent energy elastic plastic (EEEP) curves for the wall types tested.

from the average EEEP parameter calculations that were made for the average envelope of each cyclic test. All the EEEP parameters, along with their associated variability, are presented in Table 4.

Using Douglas-fir as the reference, Hinoki had a 14% increase in initial stiffness, while Sugi had a 14% decrease in initial stiffness. Douglas-fir average ultimate displacement was 73.6 mm (29 in.). The ultimate displacement of Hinoki was 4.5% higher than Douglas-fir, while for Sugi, it was 30% higher than Douglas-fir (Table 4).

Seismic equivalence parameters (SEP)

To provide a method for evaluating alternative shear wall systems, ASTM D7989-21 establishes criteria for determining equivalency to nailed, wood-frame, wood structural panel shear walls (ASTM International 2021). The average envelope curve of each specimen was used to calculate the SEPs. A shear wall configuration is considered seismically equivalent when each SEP is satisfied and when vertical load-supporting elements remain intact and capable of supporting gravity loads. The SEPs consist of component overstrength, drift capacity, and ductility. These parameters were calculated for each test and then averaged by wall type, and they require an allowable stress design (ASD) allowable shear capacity for each wall configuration. The ASD allowable shear capacity was calculated by dividing the nominal shear capacity of the wall configuration by 2.8 (American Wood Council 2020).

The nominal shear capacity was derived from Table 4.3A of the SDPWS and adjusted for specific gravity. The nominal unit shear capacity of the Douglas-fir walls was 9.78 kN/m (670 plf). For the Hinoki and Sugi walls, it was 9.30 kN/m (637 plf) and 8.41 kN/m (576 plf), respectively. The reductions in nominal

Table 4. Average EEEP parameters, along with their coefficient of variation (COV) for the wall types tested.

EEEP parameters	Douglas-fir	COV (%)	Hinoki	COV (%)	Sugi	COV (%)
P_{yield}	19.10	6.00	19.26	4.76	18.93	5.40
Δ_u (mm)	75.11	2.98	76.91	2.68	95.79	1.91
Energy (kN*mm)	1299	6.80	1360	5.17	1655	4.08
Ke (kN/mm)	1.36	14.92	1.55	14.77	1.17	20.19
$0.4*P_{peak}$ (kN)	9.32	5.54	9.52	3.05	8.87	7.28
Δ_e (mm)	6.93	9.53	6.20	11.41	7.75	18.97
Ductility ratio (m)	10.72	11.1	12.40	8.33	12.6	10.42

shear capacity for Hinoki and Sugi resulted from the specific-gravity adjustment factor noted in Table 4.3A of the SDPWS. These values were used to calculate component overstrength and ductility. The two values required for these calculations are the allowable design load (P_{ASD}) and the displacement corresponding to the allowable design load (Δ_{ASD}). Overstrength is calculated as the ratio of observed average peak load to allowable design load (P_{ASD}); drift capacity is the measure of the ultimate displacement reached of the wall; and ductility is the ratio of average ultimate displacement observed to Δ_{ASD}.

Table 5 results were derived from the average of the three cyclic wall tests per wall type. Each of the three SEPs were above prescribed target values outlined in ASTM 7989-21. Of the three SEPs, overstrength contains a lower and upper limit of 2.5 and 5.0, respectively. The upper limit exists to prevent any given component from overloading the surrounding structural elements in an actual earthquake. Each wall type met the requirements for overstrength. Furthermore, each wall type met the minimum requirement for ductility being greater than or equal to 11 and the ultimate drift being greater than or equal to 2.8% of the wall height. All wall types in this study met SEP requirements to be able to compare the results to other wall wood-based sheathed wall types in future studies.

Observed Failure Modes

Common failure of the walls was primarily fastener connection failures to the sheathing.

Fasteners were found to be either bent and pulled out of the sheathing, which occurred along the center stud of the wall or along the top and bottom of the sheathing. At the outer edges, fasteners were bent or the nail head was pulling out. Along the center stud where two sheathing panels met, nails frequently tore out the side of the OSB. This occurred because the nails were placed only 9.5 mm from the panel edge at the panel joint, which reduced the available bearing area and increased the likelihood of edge breakout. This type of behavior is a common observation in shear wall tests constructed with a single center stud (Sinha and Gupta 2009). The inner studs located at the center of the sheathing did not experience fastener failure, as the studs moved together with the panels during cyclic loading. A few walls, however, failed at the stud-to-stud connection, as shown in Figure 8.

Conclusions

Performance of shear walls framed with Sugi and Hinoki were characterized through a series of monotonic and reverse cyclic quasi-static tests. Furthermore, the performance was compared

Table 5. Seismic equivalence parameters for the wall type tested.

	Seismic equivalence parameters					
Species	Overstrength	COV (%)	Drift capacity	COV (%)	Ductility	COV (%)
DF	2.7	5.5	3.0	1.7	12.3	20.5
Hinoki	2.9	3.0	3.2	2.7	16.6	12.8
Sugi	3.0	7.2	3.9	1.9	17.4	24.5

Figure 8. Observed failure types: (a) nail pull-out; (b) nail withdrawal; (c) stud-to-stud failure.

to a standard Douglas-fir shear-wall system. Peak load of the three wall types was 31.85 kN for the Douglas-fir wall; 29.51kN for the Hinoki wall; and 23.00 kN for the Sugi wall. The initial stiffness for Hinoki was 14% higher than that of Douglas-fir framed walls, while Sugi frame walls exhibited a 30% lower initial stiffness than Douglas-fir framed walls. Within the experimental program, Hinoki walls performed similarly to Douglas-fir in terms of peak load, while Sugi walls exhibited lower peak load, initial displacement, and yield strength than Douglas-fir and Hinoki.

All walls in this study met seismic equivalence parameters defined within ASTM D7989 (ASTM International 2021). The main failure across all walls were tested occurred between the sheathing and the center stud. The distance between the nail and the edge of the sheathing at the center created a weak point in testing, exhibiting both nail head pull-through and a significant amount of nails withdrawal.

References

American Wood Council (2020) AWC Special Design Provisions for Wind and Seismic. American Wood Council.

American Wood Council (2024) AWC 2024 National Design Specification (NDS) for Wood Construction (2024 ed.). American Wood Council.

ASTM International. (2018). ASTM E564-06 Practice for Static Load Test for Shear Resistance of Framed Walls for Buildings. American Society for Testing and Materials, West Conshohocken, PA, USA. https://doi.org/10.1520/E0564-06R18

ASTM International. (2019). ASTM E2126-19 Test Methods for Cyclic (Reversed) Load Test for Shear Resistance of Vertical Elements of the Lateral Force Resisting Systems for Buildings. American Society for Testing and Materials, West Conshohocken, PA, USA. https://doi.org/10.1520/E2126-19

ASTM International. (2021). ASTM D7989-21 Standard Practice for Demonstrating Equivalent In-Plane Lateral Seismic Performance to Wood-Frame Shear Walls Sheathed with Wood Structural Panels. American Society for Testing and Materials, West Conshohocken, PA, USA. https://doi.org/10.1520/D7989-21

Bagheri MM, Doudak G (2020) Structural characteristics of light-frame wood shear walls with various construction detailing. Eng Struct 205 (Feb.):110093. https://doi.org/10.1016/j.engstruct.2019.110093

Cheung CK, Itani RY, Polensek A (1988) Characteristics of wood diaphragms: Experimental and parametric studies. Wood Fiber Sci 20(4):438–456. https://wfs.swst.org/index.php/wfs/article/view/1283

Fu J (2025, August 27). Wood-Framed Home Share Increased in 2024. National Association of Home Builders. https://eyeonhousing.org/2025/08/wood-framed-home-share-increased-in-2024/

Inayama M (2003) Design of traditional otoshikomi shear wall (in Japanese). In: Perfect menu for aseismic wooden houses. Xknoledge. Tokyo, Japan, pp 274–279.

International Code Council (2020) 2021 International Residential Code for One- and Two-Family Dwellings. International Code Council. https://codes.iccsafe.org/content/IRC2021P2

Krawinkler H, Parisi F, Ibarra LF, Ayoub A, Medina RA (2001) Development of a testing protocol for wood frame structures. CUREE - Caltech Woodframe Project Report W-02. Stanford Digital Repository. Available at: http://purl.stanford.edu/bf933wk8343

Ministry of Agriculture, Forestry and Fisheries. 2023) Annual Report on Forest and Forestry in Japan (2023). https://www.maff.go.jp/e/data/publish/AnnualReportonForestandForestry/AnnualReportonForestandForestryinJapan_FY2023_1.pdf

Mori T, Kitamori A, Komatsu K (2005) Effect of testing methods on the mechanical behavior of wooden shear walls III: consideration of wooden plate walls (in Japanese). In: Summaries of technical papers of the Annual Meeting of the Architectural Institute of Japan, C-1, structure III. Kinki, pp 399–400.

Okazaki Y, Watanabe C (2005) Shearing performance of walls that consists of Sugi lumber (in Japanese). In: Summaries of technical papers of the Annual Meeting of the Architectural Institute of Japan, C-1, structure III. Kinki, pp 333–334.

Seaders P, Gupta R, Miller TH (2009) Monotonic and cyclic load testing of partially and fully anchored wood-frame shear walls. Wood Fiber Sci 41(2):145–156. https://wfs.swst.org/index.php/wfs/article/view/473

Serrette RL, Encalada J, Juadines M, Nguyen H, Members S. (1997) Static Racking Behavior of Plywood, OSB, Gypsum, and FiberBond Walls with Metal Framing. J Struct Eng 123(8):1079–1086. https://doi.org/10.1061/(ASCE)0733-9445(1997)123:8(1079)

Sinha A, Gupta R (2009) Strain distribution in OSB and GWB in wood-frame shear walls. J Struct Eng 135(6):666–675. https://doi.org/10.1061/(ASCE)0733-9445(2009)135:6(666)

van de Lindt JW (2004) Evolution of wood shear wall testing, modeling, and reliability analysis: Bibliography. Pract Period Struct Des Constr 9(1):44–53. https://doi.org/10.1061/(ASCE)1084-0680(2004)9:1(44)

Way D, Sinha A, Kamke FA (2019) Performance of light-frame timber shear walls produced with weathered sheathing. J Archit Eng 26(1) https://doi.org/10.1061/(ASCE)AE.1943-5568.0000379